JOURNAL OF MATERIALS SCIENCE 35 (2000) 5071–5084

Heterogeneous nucleation and self-nucleation of poly(*p*-dioxanone)

M. A. SABINO, G. RONCA, A. J. MÜLLER*
Grupo de Polímeros USB, Departamento de Ciencia de los Materiales, Universidad Simón Bolivar, Apartado 89000, Caracas 1080-A, Venezuela
E-mail: amuller@usb.ve

The changes in nucleation behaviour upon addition of Boron Nitride (BN), Talc and Hydroxyapatite (HA) to poly(*p*-dioxanone) (PPDX) were monitored by DSC and Polarised Optical Microscopy (PM). Self-nucleation DSC studies evidenced the existence of the usual three self-nucleation domains depending on the self-nucleation temperature (T_s) employed. By far the best nucleation agents for PPDX were its own self-nuclei and this result was independent of the presence or absence of any of the other nucleating agents employed; once Domain II was reached, self-nucleation dominated the nucleation process. BN and Talc were able to nucleate PPDX, thereby increasing its nucleation density, its dynamic crystallisation temperature upon cooling from the melt (T_c) and its enthalpy of crystallisation (ΔH_c). BN was a better nucleating agent than talc. HA on the other hand caused an "antinucleation" effect on PPDX characterised by a decrease in its nucleation density, a decrease in its T_c and in ΔH_c. Isothermally crystallised PPDX exhibited large banded spherulites whose morphology changed as a function of crystallisation temperature from single banded structures with a very clear Maltese cross to double banded spherulites. PPDX also shows a change in growth regime upon increasing crystallisation temperature (from Regime III to Regime II) according to the kinetic interpretation of growth rate data. BN did not cause any significant modification of the spherulitic growth kinetics (in Regime II) except for a small decrease in surface free energy of PPDX crystals (σ_e). On the other hand HA was found to increase the spherulitic growth rate and the overall crystallisation rate of PPDX, this increase was caused by a degradation process experienced by the polymer during the treatments involved in isothermal crystallisation that was only present in the samples with HA. It is postulated that the interaction between the phosphate groups on the surface of HA and the ester groups of PPDX are responsible for both the antinucleation effect and the catalysis of the hydrolytic degradation of PPDX.

1. Introduction

Polydioxanone (PPDX) is a biodegradable synthetic polymer with numerous medical applications. For example, PPDX has received the approval of the Food and Drug Administration (FDA) to be used as suture material in gynaecology [1]. PPDX degrades by hydrolytic processes, generally resulting in low molecular weight molecules, which can be metabolised or bioabsorbed by the body [1–3]. PPDX has been used widely as a biodegradable suture material [3, 4]; thus, the presence of an ether bond and an additional -CH_2- in its molecular structure confer on PPDX greater flexibility in comparison to the other two frequently used biodegradable polymers, Poly(glycolic acid) (PGA) and Poly(L-Lactic Acid) (PLLA) [1, 5, 6]. Furthermore, PPDX shows lower degradation via hydrolysis, due to the lower concentration of ester groups, as compared to the aforementioned polymers [1, 3, 7]. This can lead to a longer retention of properties as a function of time. There is very limited information on the nucleation, crystallisation and morphology of PPDX in the open literature [8, 9] (in contrast for instance with PLLA [10–13]). Such information is very valuable since the degradation rate of PPDX will depend on its morphology and crystallinity as well as on its chemical structure. As far as the authors are aware, the influence of nucleating agents on the crystallisation behaviour of PPDX has not been reported.

In a previous study [9], the crystallisation and spherulitic morphology of PPDX was studied. Polarised Optical Microscopy (PM) revealed that isothermally crystallised PPDX exhibits large banded spherulites whose morphology changed as a function of crystallisation temperature from single banded well

* Author to whom all correspondence should be addressed.

developed structures with a very clear Maltese cross to double banded spherulites with a more granular texture. The morphological change occurred at a specific narrow temperature range that may correspond to a Regime III to Regime II transition according to the Lauritzen and Hoffman analysis of spherulitic growth rate data. Nevertheless, the dependence of the type of banding with crystallisation temperature may also be a consequence of a change in either crystal structure or growth axis. Avrami theory was applied to calorimetric overall crystalline conversion data and good fits were obtained with exponents ranging from 3 to 4 as isothermal crystallisation temperature was increased from 50 to 100 °C corroborating a change from instantaneous to sporadic spherulitic nucleation that was consistent with PM observations. PPDX exhibited a marked tendency to undergo partial fusion and recrystallisation during DSC heating scans.

The aim of the present paper is to study the effect of the addition of three nucleating agents on the crystallisation behaviour of PPDX and compare its effects with that of self-nucleation. The selected compounds were Hydroxyapatite (HA), Boron Nitride (BN) and Talc. It has been reported that Talc acts as an effective nucleating agent on PLLA [14] and PHB [15]. On the other hand, BN has been used to nucleate Polyhydroxybutyrate (PHB) [16]. Finally, HA is a very interesting material in view of its biocompatibility and osteoconductivity [17]. It is the main mineral constituent of teeth and bone and therefore it seems to be the most suitable ceramic material for hard tissue replacement implants although its applications in this area are still under investigation [17]. Several recent studies have tried to combine biodegradable polymers with HA in order to prepare composite materials with tailor made mechanical properties and biocompatibility for medical applications [17, 18]. HA has been used as coating material for artificial implants made of metals, ceramic or polymers with the purpose of stabilising the implant to the bone structure with minimum body rejection [17]. Its efficiency as a nucleating agent has not been established.

2. Experimental

The PPDX used in the present study was a PPDX-monofilament (Johnson & Johnson Co.). Before using PPDX, all samples were dried at 23°C under vacuum until a constant weight was achieved. This procedure is vital since humidity promotes hydrolytic degradation [2, 4, 7]. The molecular weight was obtained by capillary viscometry using phenol/1, 1, 2, 2 tetrachloro ethane (2 : 3 w/w) at 25°C. The viscosity average molecular weight M_v obtained was 1.8×10^5 g mol^{-1} using $a = 0.63$ and $K = 79 \times 10^{-3}$ cm^3 g^{-1} as Mark-Houwink parameters [7].

The nucleating agents used were Boron Nitride, BN, $CaMg(CO_3)_2$ or Talc and Hydroxyapatite (HA) with a structure of $Ca_5F(PO_4)_3$. 1 gram of PPDX was accurately weighed and mixed with the required quantity of nucleating agent at approximately 120 °C. The mixing was performed manually with a glass rod on a glass slide placed on a hot plate, while the temperature was monitored with a contact thermocouple. The homogeneity of the dispersion was checked by Polarised Optical Microscopy and found in most cases to be very good.

2.1. Polarised optical microscopy (PM)

The morphology of the PPDX films was studied with a Zeiss MC-80 polarising microscope equipped with a hot-stage Linkam TP-91 and a camera system. Thin melt-samples were prepared between microscope cover slips; they were melted at 140°C for 5 minutes and cooled at 90°C/min to the required crystallisation temperature (T_c) in the hot-stage. Spherulitic growth was followed isothermally in a wide temperature range from 50 to 100 °C. For growth rate measurements a new sample was used each time to avoid any effects due to degradation and at least two samples were measured at each T_c.

2.2. Differential scanning calorimetry (DSC)

Thermal analysis was performed with a Perkin-Elmer DSC-7 under an ultrahigh-purity nitrogen atmosphere. The equipment was calibrated with indium and tin standards. Sample weight was kept constant at 5.0 mg.

2.2.1. Dynamic DSC

In order to perform a preliminary evaluation of the thermal behaviour of the sample, dynamic heating and cooling scans were recorded at 10°C/min.

2.2.2. Isothermal crystallisation

Samples were heated to 140°C for 5 minutes to erase all previous thermal history and then were quenched (at a nominal rate of 80°C/min) to the isothermal crystallisation temperature T_c. The sample was held at T_c for the required time to develop the maximum possible crystallinity degree. Data taken during this isothermal run were used to perform the Avrami analysis.

2.2.3. Self-nucleation experiments

The extension of classical self-nucleation experiments of Blundell, Keller and Kovacs [19] to differential scanning calorimetry was conceived by Fillon, Wittmann and Lotz [20]. The procedure suggested by these authors to study self-nucleation behaviour in the DSC was applied after the sample was molten at 140°C for 5 minutes, to erase all previous thermal history; then the following protocol was followed:

a. the sample was cooled to 50°C at 10°C/min with the aim of creating a "standard thermal history";

b. the sample was again heated at the same rate up to a temperature denoted T_s or self-nucleation temperature;

c. the sample was held at T_s for 5 minutes;

d. a cooling scan of the sample was recorded from T_s down to 0°C;

e. finally, a heating scan of the sample from 0 °C up to 140 °C was recorded to register the melting behaviour.

The value of the chosen T_s is very important because it determines whether the polymer undergoes complete melting (domain I), only self-nucleation (domain II), or a combination of self-nucleation and annealing of the unmelted crystals (domain III) [20].

3. Results and discussion

3.1. The effect of nucleating agents on the dynamic crystallisation of PPDX from the melt and subsequent melting

Fig. 1 shows DSC cooling scans from the melt at a cooling rate of 10 °C/min of PPDX after keeping it at 140 °C for 5 minutes in order to erase its thermal history, for samples with and without different amounts of HA, talc or BN.

The cooling scan of PPDX without nucleating agents (Fig. 1) exhibits a crystallisation exotherm that peaks around 44 °C (see Table I). When Talc (Fig. 1) or BN (Fig. 1) is added to PPDX a clear nucleating effect can be observed that causes several effects, including a substantial increase of the onset and peak crystallisation temperatures (see Table I). The dynamic peak crystallisation temperature during cooling from the melt has been correlated with the nucleation density, and it has been shown that as the peak T_c increases the number of nuclei per volume also increases [21, 22].

In Fig. 2 the peak crystallisation temperatures upon cooling from the melt at 10 °C/min are plotted as a function of the content of nucleating agent. A similar tendency was encountered when analysing the onset crystallisation temperature, as can be seen in Table I. BN is clearly a better nucleating agent than talc, since the increase in crystallisation temperature obtained when it is added to PPDX is larger at constant composition than that obtained with talc. In both cases the nucleating effect seems to saturate as rather large amounts of the nucleating agents are incorporated in PPDX. However, the largest changes in crystallisation temperature occur below 10% addition of nucleating agent.

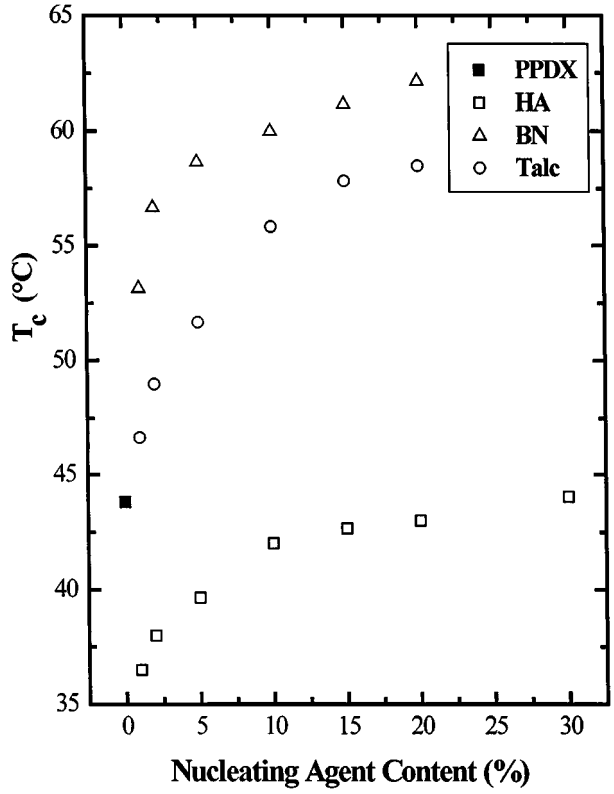

Figure 2 Peak crystallisation temperature registered during cooling from the melt at 10°C/min for neat PPDX and PPDX mixed with the indicated amounts of HA, BN and Talc.

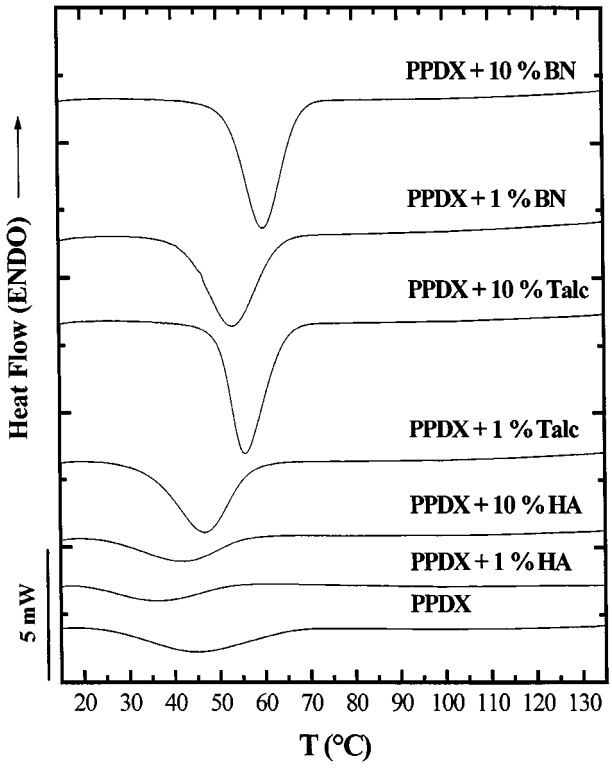

Figure 1 DSC cooling curves for neat and filled PPDX after erasing thermal history at 140 °C for 5 min, cooling rate:10°C/min.

An opposite trend to that observed with the addition of BN and talc to PPDX was observed when HA was used. An apparent "antinucleation" effect was detected as signalled by the important decrease in both the onset and peak crystallisation temperature when only 1% of the compound was incorporated in PPDX (see Fig. 1 and Table I). Fig. 2 shows that upon increasing the amount of HA, the "antinucleation" effect progressively disappears and the peak crystallisation temperature becomes the same as that of neat PPDX only at 30% addition of HA. The reason behind this antinucleation effect will be discussed below.

In the present case we are able to interpret changes in peak crystallisation temperature during dynamic cooling runs from the melt as directly related to changes in nucleation density. This correlation has been shown before for other polymers and in this case, as will be shown below, measurements were made on the nucleation density of PPDX with and without nucleating agents by PM during isothermal crystallisation and the results seem to be compatible with the efficiency of nucleation as judged by T_c increases.

In order to rate the efficiency of the three nucleating agents used here, we have employed the efficiency

TABLE I Relevant thermal transitions and enthalpies determined by DSC for PPDX and PPDX with nucleating agents

	Cooling (10 °C/min)				Heating (10 °C/min)				
Nucleant	ΔH_c (Jg^{-1})	$T_{c(onset)}$ (°C)	$T_{c(peak)}$ (°C)	ΔH_{c1} (Jg^{-1})	$T_{c1(peak)}$ (°C)	ΔH_{c2} (Jg^{-1})	$T_{c2(peak)}$ (°C)	ΔH_M (Jg^{-1})	$T_{m(peak)}$ (°C)
0%	35.1	55.3	43.8	17.4	45.0	5.20	87.0	58.3	106.8
1% HA	16.4	52.3	36.5	26.1	37.7	5.44	81.9	64.0	105.2
2% HA	20.2	53.4	37.9	23.5	37.9	4.92	81.9	60.9	105.4
5% HA	29.4	53.5	39.7	18.5	38.7	4.26	81.6	57.9	105.1
10% HA	31.6	55.7	42.0	18.1	39.2	3.59	82.7	57.2	105.5
15% HA	46.4	55.6	42.7	7.1	35.7	3.46	83.2	54.4	105.2
20% HA	41.6	55.4	43.0	7.8	35.0	3.45	83.7	52.0	105.5
30% HA	34.1	55.4	44.1	9.3	28.4	3.28	79.9	49.8	105.5
1% Talc	46.2	56.9	46.7	1.5	37.4	5.37	86.1	57.6	104.9
2% Talc	50.4	58.6	48.9	1.5	39.0	4.66	86.9	57.0	104.8
5% Talc	57.9	60.0	51.7	-	-	3.39	88.4	61.4	105.0
10% Talc	59.0	64.5	55.8	-	-	1.49	90.3	60.1	104.8
15% Talc	59.4	65.6	57.8	-	-	-	91.5	58.6	104.9
20% Talc	59.7	65.9	58.5	-	-	-	92.0	58.5	104.9
1% BN	54.9	63.4	53.2	-	-	3.55	89.0	57.0	107.2
2% BN	57.7	65.1	56.7	-	-	2.48	91.3	58.5	107.0
5% BN	60.8	67.3	58.7	-	-	1.01	91.8	60.8	106.9
10% BN	63.3	67.9	60.0	-	-	-	-	62.8	107.1
15% BN	63.4	68.5	61.2	-	-	-	-	64.7	107.0
20% BN	60.1	68.5	62.2	-	-	-	-	60.0	107.2

scale proposed by Fillon *et al*. [21]. This efficiency scale is more satisfactory than mere comparisons between peak crystallisation temperatures upon dynamic cooling from the melt, since it uses as a reference not the neat polymer but the polymer after it has been self-nucleated to saturation. Therefore a comparison with the best possible situation, i.e., when the polymer has the maximum number of ideally suited nuclei (since they are crystal fragments of identical chemical constitution and crystal lattice as the polymer) can be made.

Following Fillon *et al*. [21] the nucleating efficiency (NE) can be defined as:

$$\mathrm{NE} = 100\frac{T_{cNA} - T_c}{T_{cmax} - T_c} \quad (1)$$

Where T_{cNA} is the peak crystallisation temperature of the polymer with the nucleating agent to be evaluated, T_c is the crystallisation temperature of the neat polymer and T_{cmax} is the optimum self-nucleation temperature of the neat polymer. A detailed explanation of the self-nucleation behaviour of PPDX can be found below. It is important to note that a constant cooling rate was used to determine all these crystallisation temperatures (in this case 10 °C/min). NE is expressed as a percentage where 0 represents no nucleating action and 100 would be the ideal nucleating action.

Fig. 3 plots the NE as a function of content of nucleating agent for the three substances employed. The "antinucleation" effect of HA is now reflected in negative nucleating efficiency values that progressively increase as the HA content increases. For polymers such as isotactic Polypropylene (iPP), several nucleating agents have been found that are highly efficient with respect to their NE value (with a maximum NE of 60 to 70% [21]). However, it has also been found that small quantities of some nucleating agents are needed to saturate its NE value (i.e., even 0.1% addition of Sorbitol can already lead to a maximum efficiency in nucleating iPP [23]). The commonly used value of 1% content of nucleating agent in industry formulations is based on such experience [21].

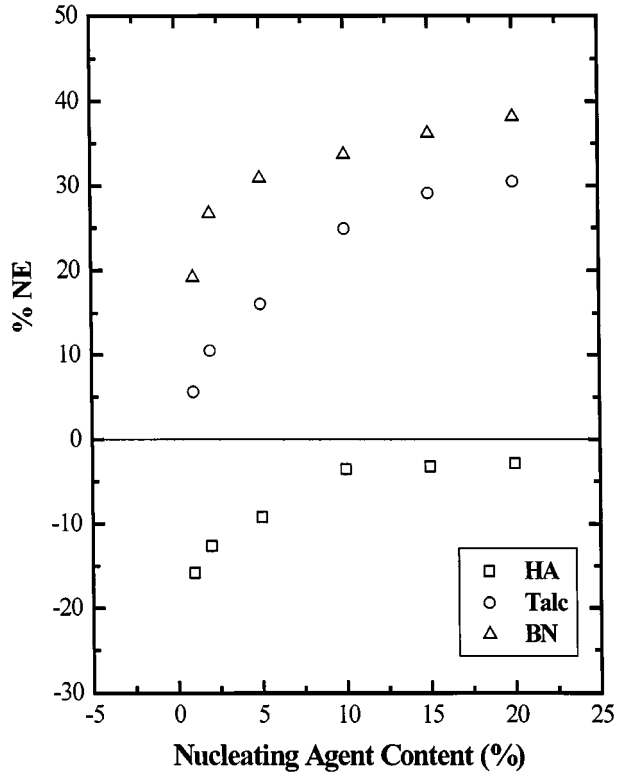

Figure 3 Nucleating Efficiency (NE) calculated according to Equation 1 for PPDX mixed with the indicated amounts of HA, BN and Talc.

In the case of PPDX, Fig. 3 shows that even with the best nucleating agent of the three employed here, BN, an efficiency of only 20% was achieved with 1% of the

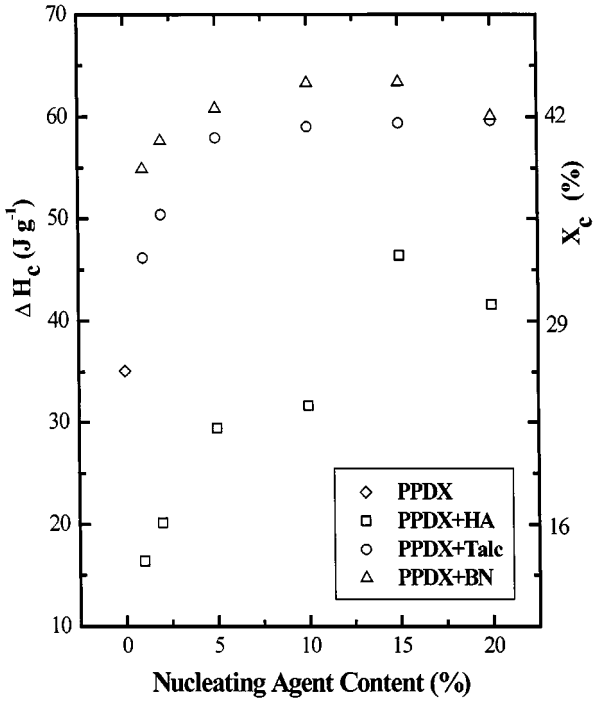

Figure 4 Crystallisation enthalpy ΔH_c and mass crystallinity degree X_c registered during cooling from subscripts the melt at 10 °C/min for neat PPDX and PPDX mixed with the indicated amounts of HA, BN and Talc.

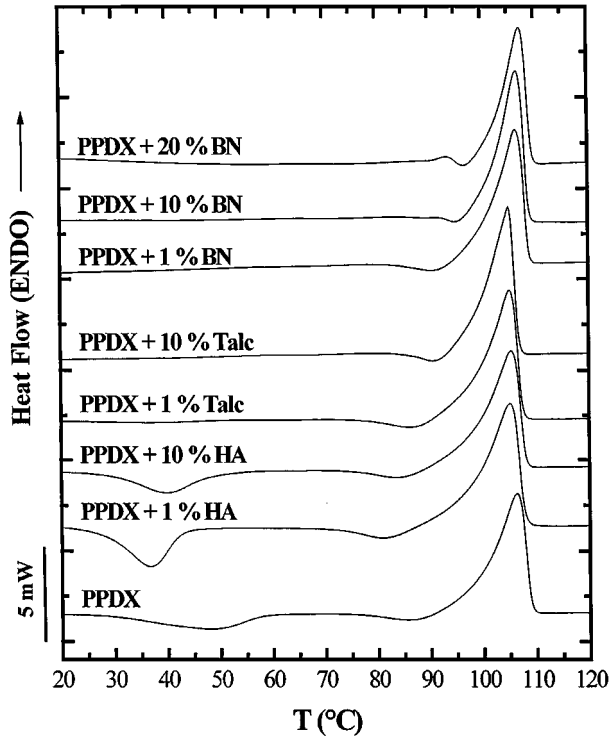

Figure 5 DSC subsequent heating curves after the cooling runs shown in Fig. 1 for neat and filled PPDX, heating rate:10°C/min.

compound. It is only when the amounts of BN approach values as high as 5–10% that NE approximates to 40%. At least with BN and talc, the maximum NE will only be achieved when the content is as high as in formulations where the nucleating agent will be considered a filler. On the contrary, with HA no apparent nucleating action could be detected in PPDX even at 30% loading.

It is interesting to analyse the effects of the nucleating agents on the maximum crystallinity achieved by PPDX during cooling from the melt. Fig. 4 displays the crystallisation enthalpy values extracted from dynamic DSC cooling runs (such as Fig. 1) as a function of nucleating agent content. PPDX is a polymer that in spite of its apparently highly flexible chemical structure only crystallises up to a value of approximately 25% crystallinity during cooling from the melt at 10 °C/min, as indicated in Fig. 4. Fig. 5 below will show that it also exhibits cold crystallisation during subsequent heating in the DSC and partial melting and recrystallisation during the scan [9]. This is why a very large effect can be produced by a nucleating agent in increasing its overall crystallinity (its value can be almost double as can be judged by the increase in ΔH_c, see Fig. 4 in a similar way to poly(ethylene terephthalate) (PET) [24].

Fig. 4 shows how BN and talc can sharply increase the crystallinity achieved by PPDX during cooling from the melt at 10 °C/min up to a maximum value located at approximately 10% nucleating agent content. This saturation trend upon increasing the content of nucleating agent is commonly observed for the majority of polymer/nucleating agents formulations [25–27].

The behaviour of PPDX with HA is also shown in Fig. 4. The compound causes a dramatic reduction in PPDX crystallinity when 1% is added. This is clearly a consequence of the reduction in T_c observed in Fig. 2 of approximately 8 °C when 1% HA is added to PPDX. It seems that the "antinucleation effect" delayed the onset of nucleation from the melt to such an extent that the overall crystallinity achieved during cooling to 0 °C was decreased. As the content of HA was increased, both T_c and ΔH_c recovered and increased to values close to that of neat PPDX. The reason why the "antinucleation effect" disappears as the content of HA increases is not clear but it may be related to the tendency of HA to form aggregates. The formation of aggregates may make difficult the dispersion of HA as its content increases and this could decrease the effective contact area between the polymer and the substrate. As a matter of fact, PM observations indicated that HA particles formed aggregates whose size was a function of HA content in PPDX. In formulations of PPDX with 30% HA, we were able to observe by PM large aggregates with sizes ranging from 50 to 100 μm.

The cooling scan of neat PPDX (Fig. 1) exhibits a crystallisation exotherm with a crystallisation enthalpy of ∼35.1 J/g (see Table I). Fig. 5 shows the subsequent heating scan for neat PPDX. We have previously shown [9] that at temperatures above the glass transition temperature (i.e., T_g is approximately 9 °C for neat PPDX) PPDX undergoes extensive reorganisation during the scan. This can be seen in Fig. 5 since two small cold crystallisation exotherms can be observed at 45°C and 87°C respectively indicating that the material did not crystallise fully during the previous cooling at 10°C/min. The enthalpy of fusion associated with the pronounced melting peak of PPDX in Fig. 5 corroborates the previous observation since its value is much higher (58.3 J/g in Table I) than the crystallisation enthalpy associated with the cooling exotherm of Fig. 1 (for neat PPDX).

Table I lists all the relevant enthalpies and temperatures evaluated from Figs 1 and 5 and other

compositions. If the crystallisation enthalpy during cooling is added to the values of ΔH_{c1} and ΔH_{c2} (i.e., the crystallisation enthalpies of the two crystallisation exotherms observed during heating and recorded in Table I) a total value of 57.7 J/g is obtained. This value is rather close to that of ΔH_m reported in Table I. In a previous work, we demonstrated by self-nucleation and isothermal crystallisation experiments that partial melting and recrystallisation should occur during the scan (possibly during and in between the two cold crystallisation exotherms in Fig. 5) for neat PPDX. Therefore, the final melting peak reflects the melting of reorganised crystals and its peak temperature only depends on the heating rate used to record the DSC scan but not on the previous thermal history of the sample [9].

Fig. 5 also shows subsequent DSC melting scans to the cooling runs shown in Fig. 1 for PPDX samples with nucleating agents. In the cases of talc and BN, the efficiency of the nucleating agents in inducing an increase in the enthalpy of crystallisation during the previous cooling runs (Fig. 4) provokes the total disappearance of the cold exotherm that is present in neat PPDX at 43.8°C (except in the case of 1% talc, although its ΔH_c value is about 10 times lower than that of neat PPDX, see Table I).

Neat PPDX exhibits a second cold crystallisation exotherm at a peak temperature of 87 °C. When talc or BN is added to PPDX (see Fig. 5) this small exotherm does not disappear completely although its ΔH_c is substantially decreased (see Table I). The peak crystallisation temperature of this second cold crystallisation exotherm shifts to higher temperatures as the nucleating agent content increases. Simultaneously, a rather broad endotherm seems to develop at temperatures just below that second cold crystallisation exotherm. As a matter of fact, in Fig. 5, when 10 and 20% BN are used, this endotherm can be seen to peak at temperatures close to 90 °C. These results indicate that even when enough active nucleating agent is added, such that PPDX can crystallise a substantial amount when cooled from the melt, the process of partial melting and reorganisation during the heating scan can still take place.

Fig. 5 shows the effect of adding HA on the subsequent heating after the cooling shown in Fig. 1. The absence of a nucleation effect in the previous cooling run (Fig. 1) is reflected in the marked cold crystallisation exotherm displayed at low temperatures during the heating DSC scans of samples containing HA in proportions less than 15% (T_{c1} in Table I).

It is rather peculiar that a nucleation effect during heating of the sample can now be observed in Fig. 5 for PPDX + HA, as far as the cold crystallisation at low temperature is concerned, since its peak crystallisation temperature (T_{c1} in Table I) is always lower for samples with HA than for neat PPDX. When crystallisable polymers like PET are used, the nucleating effect of a substance is usually manifested by raising the crystallisation temperature when cooling the polymer from the melt or by decreasing the crystallisation temperature when the same sample is heated from the glassy state [28].

The nucleation behaviour during heating of PPDX loaded with HA is difficult to explain (in view of the apparent antinucleation effect displayed by HA in Fig. 1) and may be a consequence of self-nucleation processes induced by the PPDX own crystals that were formed during previous cooling runs (as judged by the results of self-nucleation experiments presented below).

Table I also contains information on the final melting peak and enthalpy of fusion of both neat and filled PPDX. The melting point of neat PPDX is reported at 106.8 °C and does not seem to be substantially modified by the addition of the nucleating agents. In the case of BN, the difference is within the experimental error of the measurement. For both talc and HA a minor melting point depression of 1–2 °C was found. With regards to ΔH_m, most values for PPDX with nucleating agents are reasonably close to the 58.3 J/g reported for neat PPDX if the uncertainties of integrating the curves are considered (i.e., small changes in baseline and integration limits).

3.2. Self-nucleation behaviour of PPDX and PPDX with nucleating agents

Fig. 6 presents DSC curves corresponding to dynamic cooling runs at 10 °C/min of PPDX after self-nucleation at the indicated T_s temperatures. The immediate heating runs after cooling from T_s are shown in Fig. 7. In order to analyse these data; we have plotted the relevant peak crystallisation and melting temperatures as a function of self-nucleation temperatures, T_s, in Fig. 8.

Fig. 8a shows that when T_s was greater than 116 °C, the time spent at T_s was enough to erase the crystalline memory of the material, therefore PPDX needed the

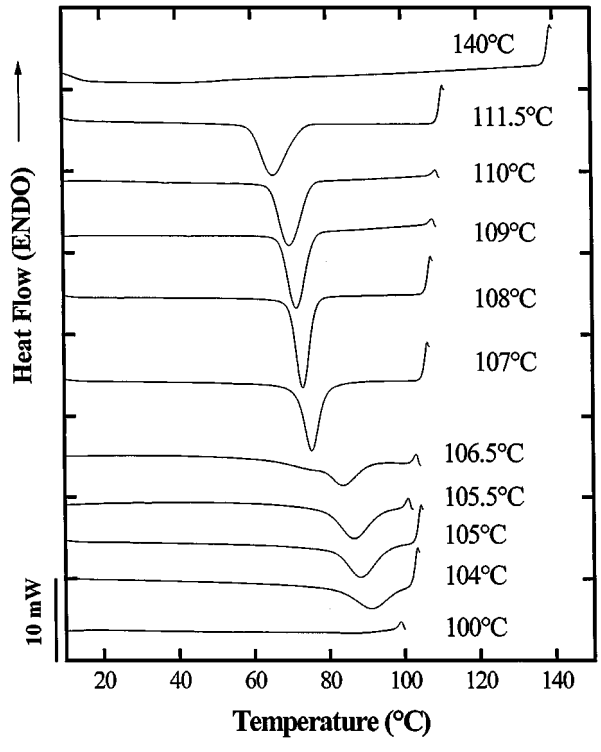

Figure 6 DSC cooling scans at 10°C/min of PPDX after 5 min at the indicated T_s temperature.

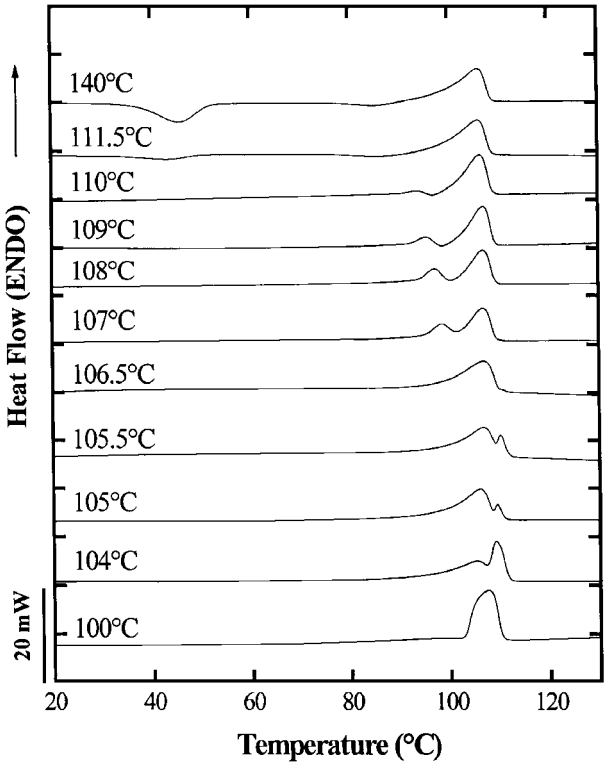

Figure 7 Subsequent DSC heating scans at 10 °C/min of PPDX after the cooling runs shown in Fig. 6, the values of T_s are indicated above each curve.

maximum undercooling in order to crystallise when cooled from T_s and the crystallisation temperature did not change with T_s. The melting point was invariant with T_s as shown in Fig. 8b when T_s was greater than 116 °C, and this was also the case for the cold crystallisation temperature of PPDX during the heating scan.

The typical behaviour of Domain I is therefore that of PPDX at $T_s > 116$ °C, where only temperature resistant heterogeneous nuclei can survive and are able to nucleate the polymer once it is cooled to the appropriate temperature [20].

A very important change in the nucleation behaviour of PPDX was found when T_s temperatures lower than 116 °C were used as indicated in Fig. 8a. This means that the boundary to Domain II or self-nucleation domain has been crossed. In this T_s temperature region, partial melting occurs leaving crystal fragments that are small enough so that annealing does not take place, but they are big enough to act as self nuclei for PPDX. The practical consequence is an enormous increase in nucleation density as T_s is lowered within the limits of Domain II [20].

Self-nucleation causes two major effects in the dynamic crystallisation of PPDX from the melt. The first effect is an expected substantial decrease in the undercooling needed for crystallisation as T_s is decreased, as can be seen in both Fig. 6 and Fig. 8a. The second effect is an increase in the enthalpy of crystallisation which is clearly seen in Fig. 6 as T_s is decreased from 140 °C to 107 °C. A similar increase in ΔH_c upon decreasing T_s has also been reported to occur in PET within Domain II [24]. In the case of iPP this effect is almost negligible since crystallisation rate is extremely fast. However in linear polyesters like PET or PPDX,

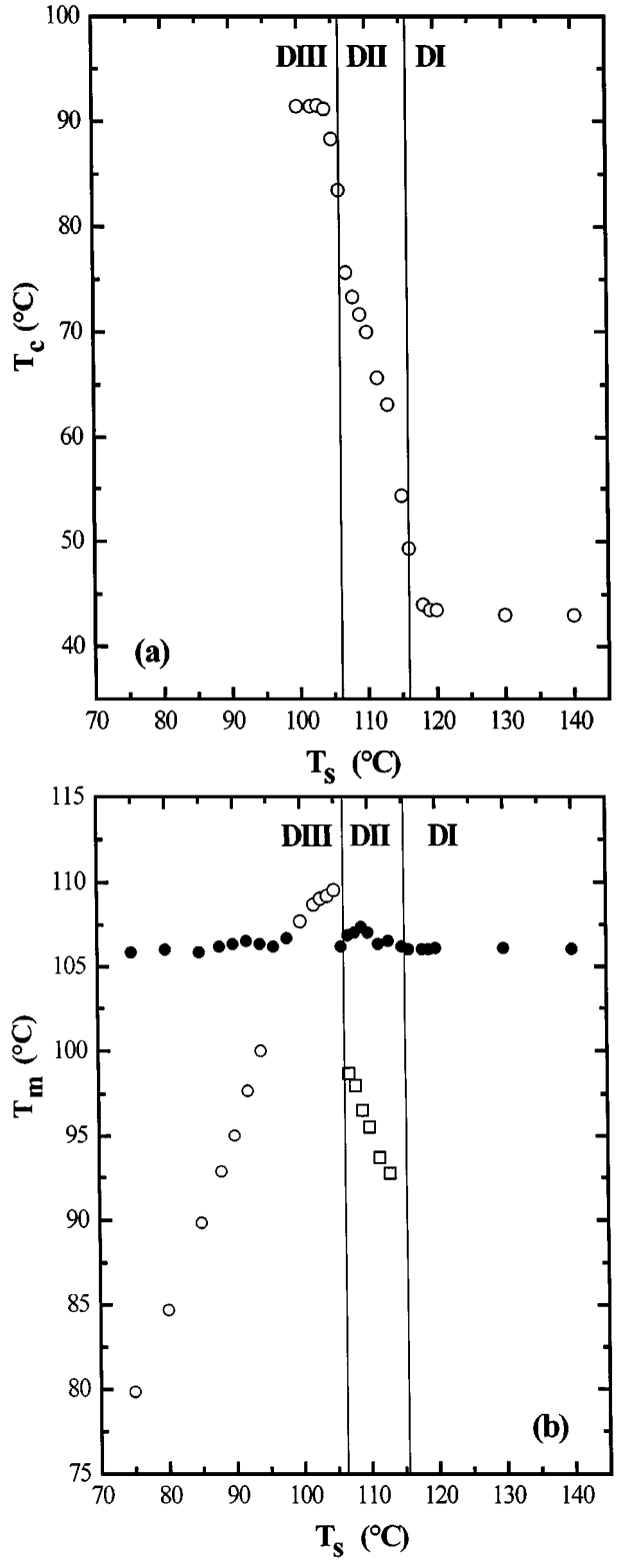

Figure 8 (a) Peak Crystallisation temperature as a function of self-nucleation temperature for PPDX (Data from Fig. 6). (b) Melting temperatures as a function of self-nucleation temperature for PPDX (Data from Fig. 7).

the substantial decrease in undercooling needed to start the crystallisation process allows the material to have a wider range between the onset T_c and T_g and therefore provides a relatively longer effective time for crystallisation during dynamic cooling from T_s at 10 °C/min.

The two effects described above for self-nucleation are very similar to that caused by the addition of BN or talc as explained in the previous section, with the

difference that the effects are somewhat smaller when these nucleating agents are used in view of their limited NE.

Fig. 7 shows heating scans after the crystallisation from T_s presented in Fig. 6. For those temperatures located within Domain II (116–106 °C) or self-nucleation domain, the lack of annealing of unmelted crystal fragments can be seen in the heating scans of Fig. 7, since there are no higher melting endotherms other than that exhibited by the material in Domain I (i.e., $T_s = 140$°C). However, two melting endotherms were observed for all the samples in Domain II in Fig. 7. The first melting temperature is highly dependent on the T_s value and occurs at lower temperatures, while the second one is practically independent of T_s and occurs at the same temperature as that exhibited by the sample whose T_s temperature was 140 °C. Fig. 8b clearly shows the T_s dependence of these two melting points within Domain II. The lower temperature melting point represents the fusion of the crystals formed during cooling from T_s while the higher temperature one is that due to the fusion of crystals that were partially melted and recrystallised during the scan, that is why its T_m values are independent of T_s [24, 28].

Finally, if T_s is decreased to temperatures below 106 °C, Domain III is reached. In this Domain, partial melting takes place but this time the amount of unmelted material is such that large crystals can survive and can experience annealing during the holding time at T_s [20]. Therefore, the transition to Domain III is best detected in the subsequent heating scans after cooling from T_s. On remelting a high temperature endotherm becomes apparent (see Fig. 7). Appearance of this high temperature shoulder (barely visible in Fig. 7 for T_s temperature 106.5°C in view of the scale used, but very clear for a T_s of 105.5°C or lower) or small peak is the trademark of domain III, i.e. of additional annealing as opposed to only self-nucleation.

The heating scans of Fig. 7 (for Domain III samples, i.e., for $T_s < 106$ °C) show complex endotherms that are composed of two signals: the endotherm that corresponds to the fusion of the crystals that were annealed at T_s, and that of the fusion of the crystals formed during cooling (and altered during the heating scan by partial melting and recrystallisation processes). Fig. 8b shows how these two T_m values depend on T_s within Domain III. The melting point that is a linear function of T_s is clearly the one corresponding to the fusion of the annealed crystals (represented in Fig. 8b by open circles). When T_s is too low, this T_m can be lower than the usual fusion temperature of the polymer (i.e., approximately 106 °C). The second melting point that is nearly independent of T_s (filled circles in Fig. 8b) corresponds to the fusion of the crystals formed during cooling (if any depending on T_s) and altered during the heating scan by partial melting and recrystallisation processes [24].

The self-nucleation experimental protocol was also applied to PPDX samples with the nucleation agents under study. The results are summarised in Fig. 9. This figure clearly shows that once self-nuclei are generated (i.e., as soon as T_s is within Domain II), these self-

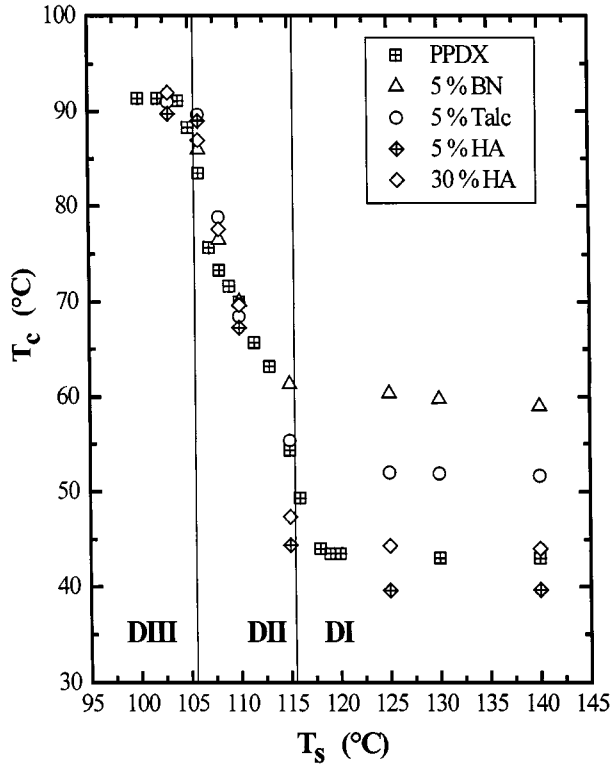

Figure 9 Peak Crystallisation temperature as a function of self-nucleation temperature for neat PPDX and PPDX mixed with the indicated amounts of HA, BN and Talc.

nuclei preferentially nucleate PPDX regardless of the type and content of the nucleating agent employed. This result was expected since the best nucleating agent for PPDX should be its own crystals (they would have a 100% NE value). It is interesting to point out that even the antinucleating effect of HA disappears when a T_s temperature within domain II is used, even though it is clearly present in Domain I when the PPDX is fully melted at the T_s temperatures used in Domain I.

3.3. Influence of nucleating agents on the isothermal crystallisation behaviour of PPDX

A detailed description of PPDX spherulites can be found in a previous work, where isothermal crystallisation of PPDX was studied [9]. When PPDX is crystallised from the melt it forms banded spherulites that can exhibit a well defined Maltese cross depending on the crystallisation temperature. The variation in band spacing with T_c and the temperature dependence of mean spherulite diameter are both increasing functions of the crystallisation temperature and resemble the behaviour reported for Polyhydroxybutyrate, PHB [29], Poly(ε-Caprolactone) and Polyamides [30].

At large undercoolings well-defined spherulites (with very clear banding and Maltese cross extinction patterns) were observed for neat PPDX crystallisation temperatures between 60 and 75 °C. As the undercooling was reduced several changes in the spherulitic morphology were observed. At crystallisation temperatures of 80 °C or higher the spherulites exhibit "double

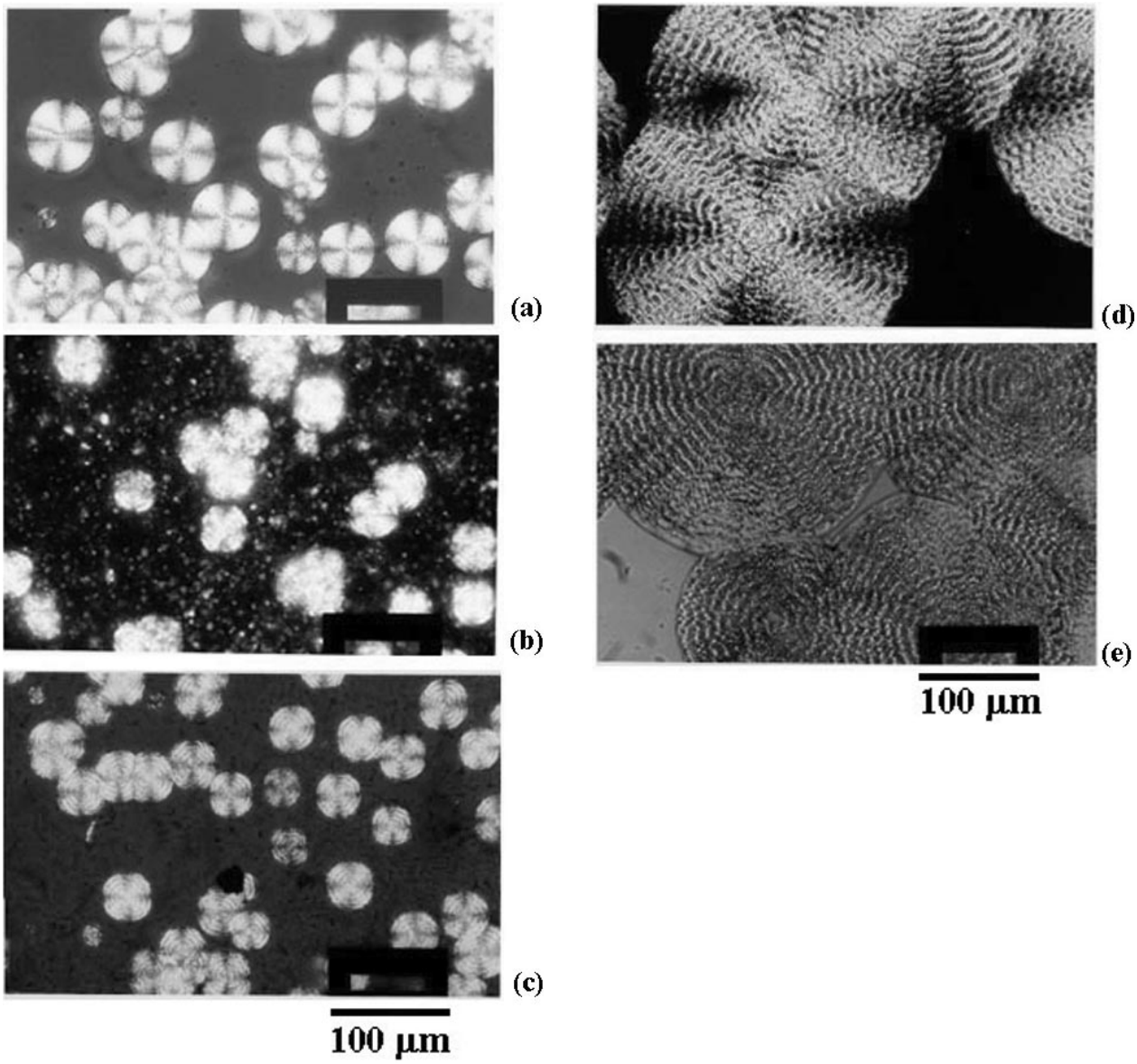

Figure 10 Polarised optical micrographs showing spherulites growing at 75 °C of: (a) neat PPDX, (b) PPDX + 1%HA, (c) PPDX + 1% BN; and spherulites growing at 85 °C of: (d) neat PPDX and (e) PPDX + 1% HA.

banding", a banding with two different periodicities whose mean distance between these double rings nevertheless keeps increasing with T_c. This double banding also resembles that encountered in several aliphatic polyesters or in PHB spherulites [29, 31–33]. The origin of ringed spherulites was studied in detailed by Keller [33, 34] and by Keith and Padden [31, 32]. The single ring extinction patterns in polymer spherulites have been interpreted as arising from a uniaxial indicatrix twisted about a normal to the optic axis (i.e., like in polyethylene, a polymer that has an orthorhombic unit cell and approximates very closely a uniaxial material). Doubled ringed spherulites arise when the material possesses a biaxial indicatrix twisted about the optic normal leading to uneven spacing of the rings. The morphological change experienced by PPDX upon increasing T_c may be due to a change in crystal structure or growth axis in view of the change in the extinction patterns.

The morphological change in PPDX with increasing crystallisation temperature (i.e., from single to double-ringed spherulites) occurred at a specific narrow temperature range (75–80 °C) that also coincided with a Regime III to Regime II transition according to the Lauritzen and Hoffman analysis of spherulitic growth rate data [9]. This may be just a coincidence and further evidence should be obtained in future studies to clarify this point and determine whether a change in crystal structure or growth axis is simultaneously occurring.

Fig. 10 shows a series of optical micrographs of PPDX spherulites grown at 75 °C and 85 °C (with and without nucleating agents). If a comparison is made of the number of growing spherulites at 75 °C between the neat PPDX and that with 1% BN or with 1% HA, it is clear that the nucleation density is increased by the use of BN but decreased by the use of HA. It should be mentioned that the birefringent particles in Fig. 10b of sizes less than 10 μm are not small spherulites but HA aggregates since they were always present (even at 120 °C) and did not experience any growth with time. The size of these HA aggregates depended on the HA content as mentioned above.

Fig. 11 presents an approximate estimation of the nucleation density that was made from PM observations as a function of time. Fig. 11 shows the usual trend

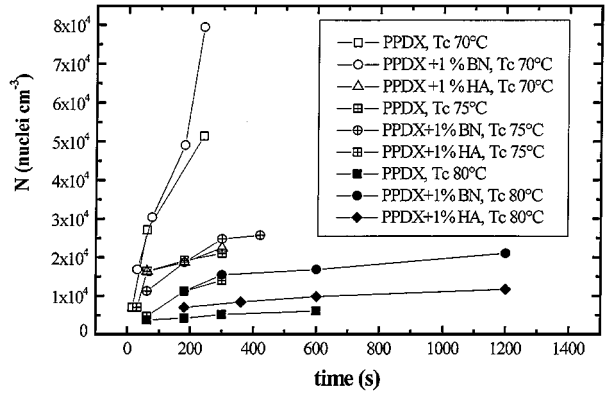

Figure 11 Nuclei concentration as a function of time for neat PPDX and PPDX mixed with the indicated amounts of HA, BN and Talc.

of increasing the number of nuclei per unit volume as crystallisation time elapses. It also shows that at lower crystallisation temperatures (70 or 75 °C) the nucleation density seems to follow the order of NE suggested in Fig. 3, thereby the direct relationship between T_c and nucleation density suggested above is plausible also in this case.

It is important to note that HA seems to be causing a genuine "antinucleation" effect on PPDX since not only T_c is depressed (Fig. 2) by the incorporation of 1% HA but the actual number of active nuclei also decreases. In morphological terms, the spherulites of neat PPDX or those nucleated by HA are very similar, as shown in Fig. 10, they even show the characteristic double banding at high crystallisation temperatures (see examples at 85 °C in Fig. 10d and e). However, there are minor differences, since spherulites of PPDX + 1% HA seem to be slightly coarser and their Maltese crosses are not so well defined (see for example Fig. 10b, and in particular the samples crystallised at 85 °C in Fig. 10e, where more details are apparent) as in neat PPDX.

Spherulitic growth rates were calculated after measuring spherulitic radii from sequential polarised optical micrographs as a function of time. The radial growth rates were found to be linear in all cases. The kinetics were followed for neat PPDX and for PPDX loaded with 1% BN or 1% HA. Fig. 12 presents the variation of spherulitic growth rate as a function of crystallisation temperature. Crystallisation temperatures lower than 50 °C caused very fast growth of small spherulites that quickly impinged with one another making growth measurements very difficult to make in neat PPDX.

Fig. 12 corroborates that BN is acting as a classical nucleating agent, since it does not affect the rate at which spherulites grow. Its action is limited to the creation of new nucleation sites that are active at lower supercoolings than those needed for the usual heterogeneities present in PPDX to become active. Therefore, BN produces an increase in nucleation density (Fig. 11) and an increase in the peak crystallisation temperature when PPDX is crystallised from the melt (Figs 1–3). This increase in nucleation density resulted in smaller spherulites (Fig. 10), the reason behind the absence of data for temperatures lower than 70 °C in Fig. 12. However, once the nuclei are activated, the spherulite growth that follows is produced at the same rate as that of PPDX

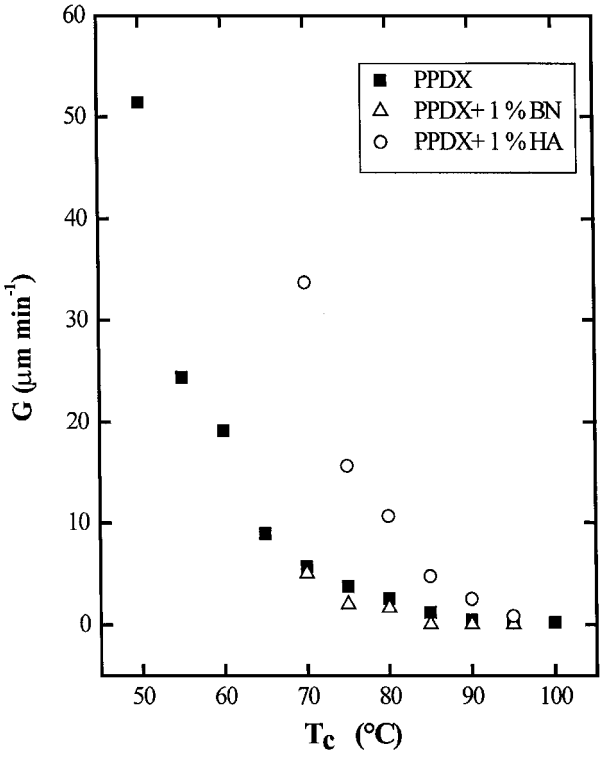

Figure 12 Variation in spherulite growth rate with crystallisation temperature for neat PPDX and PPDX mixed with 1% of HA or BN.

when the comparison is made at the same isothermal crystallisation temperature (Fig. 12).

In contrast to BN, the behaviour of HA was again not the expected one. Fig. 12 shows that the sample of PPDX with 1% HA exhibited a faster crystallisation rate than neat PPDX, especially at lower temperatures (in this case this is the reason behind the lack of experimental data below 70 °C in Fig. 12). This behaviour is clearly unexpected, specially when HA induces an apparent antinucleation effect on PPDX.

Earlier reports of antinucleation phenomena indicate that "antinucleating agents" seem to reduce crystallisation rate. For instance, it has been reported that amounts of silica nucleants in excess of 5% reduce the crystallisation rate of PET in spite of increasing nucleation density [35, 36]. This has been interpreted as being due to an increase in melt viscosity produced by a strong interaction between PET and silica. Another example is provided by Mercier [37] who reports that the central Na sulfonation of PEK (an aromatic polyetherketone) results in antinucleation effects that included the reduction of both the crystallisation temperature during dynamic crystallisation and a slow down of the crystallisation rate. A different type of antinucleation has been also recently reported by Balsamo *et al*. [38] for the Polycaprolactone block of SEC block copolymers (Polystyrene-Polyethylene-Polycaprolactone). However in that case, the antinucleation effect had its origins in topological constrains induced in the PCL block by the PE crystals within the PE block when they were annealed [38].

If the kinetic theory of polymer crystallisation is used to analyse the spherulitic growth rate data the values for surface energies within the crystals can be

obtained. Hoffman [39, 40] gives the linear growth rate of spherulites as:

$$G = G_0 \exp\left[\frac{-U^*}{R(T_c - T_\alpha)}\right] \exp\left[\frac{-K_g}{(T_c \Delta T f)}\right] \quad (2)$$

where G_0 is a rate constant, U^* is an activation energy for the transport of molecules to the growth front, R is the gas constant, T_α is the temperature below which molecules become immobile (usually approximated to $T_\alpha = T_g - 30$), K_g is a kinetic constant for the secondary nucleation, T_c is the crystallisation temperature, ΔT is the supercooling ($T_m^0 - T_c$), T_m^0 is the equilibrium melting temperature and f is a correction factor that accounts for the change of heat of fusion as the temperature is decreased below T_m^0 (f is equal to $2T_c/(T_m^0 + T_c)$).

In order to apply the treatment of Lauritzen and Hoffman, we have used the following values: $U^* = 6300$ J/mol, $T_\alpha = -40^\circ$C and $T_m^0 = 127.1^\circ$C [8, 9]. Fig. 13 shows a plot of $\ln G + U^*/R(T_c - T_\alpha)$ versus $1/(T_c \Delta T f)$ for neat PPDX and PPDX with 1% HA and 1% BN. There is a clear change in slope in Fig. 13 for neat PPDX that has been interpreted as a change in growth regime [41–44]. PPDX samples are crystallising in regime RII (at low supercoolings) and then change to regime RIII (at large supercoolings), the transition temperature is located in the range 75–80°C. An additional evidence of a regime II–III transition can be obtained by the ratio of the slopes $K_{g(RIII)}/K_{g(RII)}$ since a result close to 2 was found (i.e., 2.2, see ref. [9]). A similar Regime II–III transition was also found by Barham *et al*. using PHB [29, 45] and by Iannace and Nicolais for PLLA [11] among others [42]. As previously indicated, the temperature of the regime II–III transition corresponds to the limit at which single banding is observed [9].

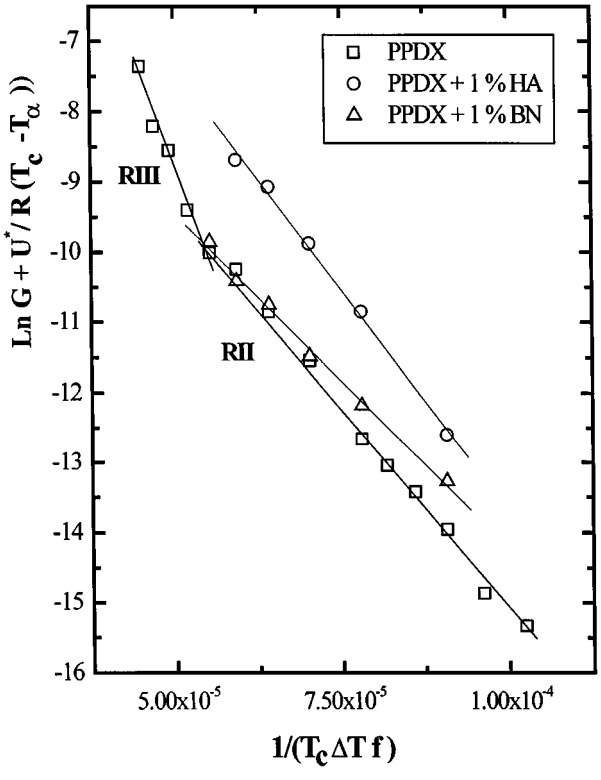

Figure 13 Plots of $\ln G + U^*/R(T_c - T_\alpha)$ as a function of $1/(T_c \Delta T f)$ for neat PPDX and PPDX mixed with 1% of HA or BN.

In the case of both BN and HA filled PPDX samples, Fig. 13 shows that both samples seem to be under Regime II since no substantial differences in slope can be observed. Unfortunately, no data are available at high supercoolings where the change to Regime III was detected for PPDX for the reasons already explained above. The fact that spherulitic growth is faster when HA is present accounts for the displacement of the $\ln G + U^*/R(T_c - T_\alpha)$ values for PPDX + 1% HA to higher values as compared to neat PPDX.

The slopes (K_g) of the secondary nucleation analysis can be used to estimate the fold surface free energies, σ and σ_e, of the polymer:

$$K_g = \frac{j b_0 \sigma \sigma_e T_m^0}{(k \Delta H_f)} \quad (3)$$

where b_0 is the width of the chain; ΔH_f^0 is the heat of fusion of a 100% crystalline sample, j is determined by the operating regime and is equal to 4 for regime I and III, and equal to 2 for regime II, k is Boltzmann's constant and σ and σ_e are the lateral and fold surface free energies, respectively. The values of a_0 and b_0 ($a_0 b_0$ is the molecular area of the chain) were taken as 0.45 nm and 0.41 nm [46], which are the values reported for Poly(ε-caprolactone), PCL, since no data are available for PPDX and the molecular structure of PPDX is similar to that of PCL. The ΔH_f^0 value was reported by Ishikiriyama *et al*. [8] as 14.4 kJ mol^{-1}. The values of $\sigma \sigma_e$ can then be determined from the slope of the lines in Fig. 13 and the results are presented in Table II.

The Hoffman modification of the Thomas-Stavely relation [46, 47] was employed to estimate σ:

$$\sigma = 0.1 \Delta H_f^0 [a_0 b_0]^{1/2} \quad (4)$$

a value of 8.556 (mJ/m^2) for σ was obtained. Using this value an estimate of the fold surface free energy (σ_e) was calculated and reported in Table II. Once σ_e was obtained, the work done by the PPDX chain (q) to form a fold was calculated by:

$$q = 2 a_0 b_0 \sigma_e \quad (5)$$

Table II also reports the calculated q values. The values obtained in Table II are within the range usually encountered for flexible linear macromolecules [46].

TABLE II Isothermal Crystallisation Kinetic parameters obtained from spherulitic growth rate data

	PPDX		PPDX + 1% BN	PPDX + 1% HA
	RII	RIII	RII	RII
$K_g \times 10^{-5}$(K^2)	1.19	2.49	0.96	1.27
$\sigma\sigma_e \times 10^6$ (J^2/m^4)	619.3	644.7	494.1	684.3
$\sigma_e \times 10^3$ (J/m^2)	72.4	75.3	57.8	79.9
$q \times 10^6$ (J)	2.67	2.78	2.13	2.95
Ln G_0 (G_0 in μm/s)	−3.19	3.68	−4.67	−1.05
structure			spherulitic	

The effect of the addition of BN or HA does not seem to affect greatly the growth rate kinetics under Regime II. A lower value of σ_e was obtained for the sample nucleated with BN, a fact consistent with Beck's criterion. According to the work of Beck [48, 49], a good nucleating agent should reduce the interfacial surface free energy. Table II shows that only with BN a reduction of σ_e was obtained (and an expected decrease in q), since HA produced a slightly higher value of σ_e than that of neat PPDX.

3.4. Overall crystallisation kinetics

We have used Avrami's equation to analyse the isothermal crystallisation calorimetric data obtained by DSC [46, 47]:

$$1 - v_c(t) = \exp[-Kt^n] \quad (6)$$

where n is known as the Avrami index, K is a rate constant and v_c (t) is the relative crystalline fraction of the polymer. In general n and K characterise the nucleation type and the crystal growth geometry, this index usually varies between 3 and 4 for semi-crystalline polymers [46, 47].

The values of n and K derived from applying Avrami equation to isothermal crystallisation data obtained by DSC are shown in Table III. A previous study comprising crystallisation temperatures from 30 to 80 °C has shown a systematic increase in Avrami index from approximately 2 to 3.8 [9]. Table III only contains data for a limited crystallisation temperature range where n for PPDX varies between 3.1 to 3.8. This behaviour is typical of semi-crystalline polymers and is due to the increasingly sporadic nature of the nucleation process as the crystallisation temperature is raised [50].

The effect of adding BN and HA on the values of K, n is presented in Table III. Since Avrami's treatment comprises both the nucleation and the growth of crystals, it can be difficult to interpret.

In the case of the addition of BN, a decrease in Avrami's index is expected since the nucleation of three dimensional spherulites (Fig. 10) should be more instantaneous as compared with neat PPDX (Fig. 11). Table III indeed shows lower values of n for PPDX + 1overall crystallisation rate (nucleation and growth) may also be expected with the addition of BN (since nucleation is enhanced) and is also observed in Table III when K values are compared.

TABLE III Avrami coefficients for PPDX as a function of isothermal crystallisation temperature

Sample	T_c (°C)	n	K (s^{-n})
PPDX	60	3.39	9.38×10^{-7}
	70	3.56	3.22×10^{-7}
	80	3.77	1.35×10^{-7}
PPDX + 1% HA	60	3.12	3.21×10^{-5}
	70	3.19	2.55×10^{-6}
	80	3.15	1.41×10^{-6}
PPDX + 1% BN	60	3.09	7.51×10^{-7}
	70	3.17	2.07×10^{-7}
	80	3.22	1.01×10^{-7}

For HA the situation is complex since, as it has been shown it slows down nucleation but enhances spherulitic growth rate of PPDX. Therefore the overall crystallisation rate of PPDX + HA may be difficult to predict. According to Table III, the values of K, the overall conversion rate are higher than for pure PPDX indicating that once again when isothermal crystallisation is considered, the increase in crystallisation rate dominates over the decrease in nucleation rate.

3.5. The behaviour of PPDX with HA

As can be gathered from the results presented above, the behaviour of PPDX with HA is very peculiar. The effect caused by HA on the nucleation and crystallisation of PPDX seems to be a result of the competition of two processes. On one hand the compound clearly causes an antinucleation effect that manifests itself by decreasing nucleation density and causing a depression in dynamic T_c and a reduction in the crystallinity degree achieved during cooling from the melt. On the other hand, HA increases the isothermal spherulitic growth of PPDX and the overall crystallisation rate.

It is clear that when a dynamic experiment is performed, such as those depicted in Fig. 1, the antinucleation effect dominates over the possible increase in crystallisation rate. This may be caused by a reduction in the crystallisability window (i.e., difference between crystallisation onset at 10 °C/min and vitrification) due to the substantial decrease in T_c, nevertheless other factors may also play an important role as explained in what follows.

The possible interactions between HA and PDDX may arise from the presence of phosphate groups in HA. The biodegradability of PPDX stems from its susceptibility to undergo hydrolytic degradation. The hydrolysis usually occurs via the ester bond yielding alcohol and carboxylic acid groups. Furthermore, hydrolytic degradation studies have been performed in several biodegradable aliphatic polyesters, like PGA [51, 52], PLLA [53] or even PPDX [7]. These studies have shown that phosphate ions can catalyse the hydrolytic degradation of the ester groups in these polyesters causing substantial decreases in hydrolytic degradation time.

The effect of hydrolytic degradation on the crystallisation kinetics of PPDX has been the subject of a parallel study in our laboratory [54]. In the course of that study, PPDX samples were immersed in phosphate buffer solutions for several weeks. After 6 or 12 weeks the samples were dried and their spherulitic morphology and crystallisation kinetics was examined. A substantial increase in spherulitic growth rate was detected for samples whose molecular weight was reduced from 18.0000 g/mol to 19.000 g/mol in 12 weeks of treatment.

In view of all of the above, it is possible that phosphate groups in HA are catalysing a possible hydrolytic degradation in PPDX, in spite of the careful drying procedure of both PPDX and HA before mixing. It may be possible that during the mixing procedure, which was performed on air, some moisture may have been absorbed by HA and PPDX. In order to test this hypothesis

the samples with 1% HA that were used for the determination of spherulitic growth rates were carefully dissolved in a mixture of phenol and tetrachloroethane and filtered twice to remove the HA. After this process was completed, the viscosity average molecular weight of PPDX was once again measured. It was found that M_v decreased from 180.000 g/mol for neat PPDX to 130.000 g/mol for the PPDX that was in contact with HA during the thermal treatments needed to measure its isothermal spherulitic growth rate or overall crystallisation kinetics.

The result presented above explains why the spherulitic growth rate is enhanced during isothermal crystallisation, while during dynamic crystallisation at 10 °C/min this is not so apparent. It is clear that during isothermal crystallisation the time PPDX spends at higher temperatures is greater than that during dynamic cooling from the melt.

The antinucleation effect of HA on PPDX may also be linked to the interactions between the phosphate groups on the surface of HA and PPDX. As explained above, the mechanism for hydrolytic degradation (see reaction scheme below) involves the initial hydrolysis of the ester group followed by the formation of a complex between the hydrolysed PPDX molecule and the phosphate ions that can form on the surface of the HA particles. The formation of this complex may limit the local mobility of PPDX chains and may be responsible for the antinucleation effect. These complexes are highly unstable and they will cause chain scission of PPDX molecules (as indicated in the proposed reaction scheme), a fact that increases

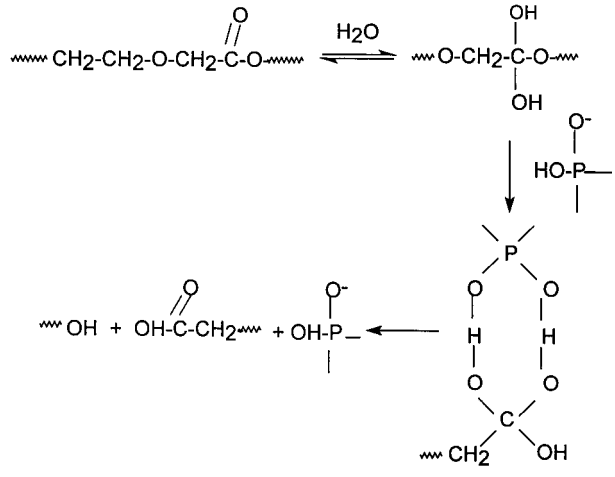

chain mobility and therefore the crystallisation kinetics. The competition between these two opposing effects may be causing the observed behaviour.

The results obtained in the present study may be of interest for the production of bioabsorbable implants (for example in the production of pins used for bone fracture treatments), since HA could reduce the time the human body needs to biodegrade PPDX and is also biocompatible as stated in the introduction.

4. Conclusions

Self-nucleation studies evidenced the existence of the usual three self-nucleation domains in PPDX depending on the self-nucleation temperature (T_s) employed. By far the best nucleation agents for PPDX were its own self-nuclei and this result was independent of the presence or absence of any of the other nucleating agents employed. It was demonstrated that once Domain II was reached, self-nucleation dominated the nucleation process.

BN and Talc were able to nucleate PPDX, thereby increasing its nucleation density, its dynamic crystallisation temperature upon cooling from the melt (T_c) and its enthalpy of crystallisation (ΔHc). BN was a better nucleating agent than Talc displaying a greater "Nucleating Efficiency" (NE). HA on the other hand caused an "antinucleation" effect on PPDX characterised by a decrease in its nucleation density, a negative NE and a reduction in ΔH_c.

Isothermally crystallised PPDX exhibited large banded spherulites whose morphology changed as a function of crystallisation temperature from single banded structures with a very clear Maltese cross to double banded spherulites. The change in banding coincided with a change in growth regime according to the kinetic interpretation of spherulitic growth rate data.

BN did not cause any significant modification of the spherulitic growth kinetics (in Regime II) except for a small decrease in surface free energy of PPDX crystals (σ_e). On the other hand HA was found to increase the spherulitic growth rate of PPDX and its overall crystallisation rate, this increase was caused by a degradation process experienced by the polymer during the thermal treatments involved in isothermal crystallisation that was only present in the samples with HA. It is postulated that the interaction between the phosphate groups on the surface of HA and the ester groups of PPDX are responsible for both the antinucleation effect and the catalysis of the hydrolytic degradation of PPDX.

Acknowledgements

The authors would like to thank the "Decanato de Investigación *y* Desarrollo" from USB and CONICIT (S1-95000711) for giving their financial support to make this project possible.

References

1. C. ELVIRA, A. GALLARDO, J. SAN ROMAN and A. LÓPEZ, *Revista de Plásticos Modernos* **77** (1999) 49.
2. S. KARLSSON, M. HAKKARAINEN and A. C. ALBERTSSON, *J. Chromatography* **688** (1994) 251.
3. C. C. CHU, *J. Appl. Polym. Sci.* **26** (1981) 1727.
4. J. A. RAY, N. DODDI, D. REGULA, J. A. WILLIAMS and A. MELVEGER, *A. Surg. Gyn. Obst.* **153** (1981) 497.
5. M. CANETTI, M. URSO and P. SADOCCO, *Polymer* **40** (1999) 2587.
6. Z. GAN, D. YU, Z. ZHONG, Q. LIANG and X. JING, *ibid.* **40** (1999) 2859.
7. M. A. SABINO, L. MARZIN and J. L. FEIJOO, *Revista Técnica de Ingeniería de la Universidad del Zulia* **21** (1998) 170.
8. K. ISHIKIRIYAMA, M. PYDA, G. ZHANG, T. FORSCHNER, J. GREBOWICZ and B. WUNDERLICH, *J. Macromol. Sci-Phys.* **B37** (1998) 27.
9. M. A. SABINO, J. L. FEIJOO and A. J. MÜLLER, *Macromol. Chem. Phys.*, accepted for publication.
10. M. F. GONZÁLEZ, R. A. RUSECKAITE and T. CUADRADO, *J. Appl. Polym. Sci.* **71** (1999) 1223.

11. S. IANNACE and L. NICOLAIS, *ibid.* **64** (1997) 911.
12. T. MIYATA and T. MOSUKO, *Polymer* **39** (1998) 5515.
13. R. J. ZWIERS, S. GOGOLEWSKI and A. J. PENNINGS, *ibid.* **24** (1983) 175.
14. J. KOLSTAD, *J. Appl. Polym. Sci.* **62** (1996) 1079.
15. P. J. BARHAM, *J. Mater. Sci.* **19** (1984) 3826.
16. D. VESELY and G. RONCA, *Inst. Phys. Conf. Ser.* **78** (1985) 423.
17. W. SUCHANEK and M. YOSHIMURA, *J. Mater. Res.* **13** (1998) 94.
18. K. DE GROOT, *J. Ceramics Soc. Japan* **99** (1991) 917.
19. D. J. BLUNDELL, A. KELLER and A. J. KOVACS, *J. Polym. Sci.* **B4** (1966) 481.
20. B. FILLON, J. C. WITTMAN, B. LOTZ and A. THIERRY, *J. Polym. Sci, Polym.-Phys.* **31** (1993) 1383.
21. B. FILLON, B. LOTZ, A. THIERRY and J. C. WITTMANN, *ibid.* **31** (1993) 1395.
22. G. EDER, H. JANESCHITZ-KRIEGL and S. LIADANER, *Prog. Polym. Sci.* **15** (1990) 629.
23. A. MANAURE and A. J. MÜLLER, *Macromol. Chem. Phys.* **201** (2000) 958.
24. C. H. MOLINUEVO, G. A. MENDEZ and A. J. MÜLLER, *J. Appl. Polym. Sci.* **70** (1998) 1725.
25. H. N. BECK and H. D. LEDBETTER, *ibid.* **9** (1965) 2131.
26. H. N. BECK, *J. Appl. Polym. Sci.* **11** (1987) 673.
27. F. L. BINSSBERGEN, *Polymer* **11** (1970) 253.
28. E. A. TURI ed., "Thermal Characterization of Polymeric Materials," 2nd ed. (Academic Press, New York, 1997).
29. P. J. BARHAM, A. KELLER, E. L. OTUM and P. A. HOLMES, *J. Mater. Sci.* **19** (1984) 2781.
30. H. D. KEITH, F. J. PADDEN and T. P. RUSSEL, *Macromolecules* **22** (1989) 666.
31. H. D. KEITH, F. J. PADDEN, *J. Polym. Sci.* **39** (1959) 101.
32. *Idem., ibid.* **39** (1959) 123.
33. A. KELLER, *ibid.* **39** (1959) 151.
34. *Idem., ibid.* **17** (1955) 291.
35. G. TURTURRO, G. R. BROWN and L. E. ST. PIERRE, *Polymer* **25** (1984) 659.
36. S. CHENG and R. A. SHANKS, *J. Appl. Polym. Sci.* **47** (1993) 2149.
37. J. P. MERCIER, *Polym. Eng. Sci.* **30** (1990) 270.
38. V. BALSAMO, A. J. MÜLLER and R. STADLER, *Macromolecules* **31** (1998) 7756.
39. J. D. HOFFMAN, G. T. DAVIS and J. L. LAURITZEN JR, in "Treatise on Solid State Chemistry," edited by N. B. Hannay (New York, 1976), Ch. 7.
40. J. D. HOFFMAN, *Polymer* **23** (1982) 656.
41. *Idem., ibid.* **24** (1983) 1.
42. J. D. HOFFMAN and R. L. MILLER, *Macromolecules* **22** (1989) 3501.
43. J. XU, S. SRINIVAS, H. MARAND and P. AGARWAL, *ibib.* **31** (1998) 8230.
44. J. D. HOFFMAN and R. L. MILLER, *Polymer* **38** (1997) 3151.
45. S. J. ORGAN and P. J. BARHAM, *J. Mater. Sci.* **26** (1991) 1368.
46. K. MEZGHANI and P. J. PHILLIPS, in "Physical Properties of Polymers-Handbook," edited by J. E. Mark (AIP Press, New York, 1996) Ch. 31.
47. U. W. GEDDE, in "Polymer Physics" (Chapman & Hall, London, 1995) p. 169.
48. H. N. BECK, *J. Appl. Polym. Sci.* **19** (1975) 371.
49. Y. FENG, X. JIM and J. N. HAY, *ibid.* **69** (1998) 2089.
50. F. P. PRICE, in "Nucleation," edited by A. C. Zettlemoyer (New York, 1969) Ch. 8.
51. D. F. WILLIAMS, *J. Mat. Sci.* **17** (1982) 1233.
52. C. C. CHU, *Polymer* **26** (1985) 591.
53. C. A. P. JOZIASSE, D. W. GRIPMA, J. E. BERSMA, F. W. CORDEWENER, R. R. M. BOS and A. J. PENNINGS, *Colloid Polym. Sci.* **276** (1998) 968.
54. M. A. SABINO, J. L. FEIJOO and A. J. MÜLLER, to be published.

Received 31 January
and accepted 6 March 2000